# Cytochrome P450-Dependent Lipid Metabolism in Preovulatory Follicles

J. W. NEWMAN, J. E. STOK, J. D. VIDAL, C. J. CORBIN, Q. HUANG, B. D. HAMMOCK, AND A. J. CONLEY

*Department of Entomology (J.W.N., J.E.S., Q.H., B.D.H.), University of California-Davis Cancer Research Center (J.W.N., J.E.S., Q.H., B.D.H.), and Department of Population Health and Reproduction (J.D.V., C.J.C., A.J.C.), University of California, Davis, California 95616*

Estrogen biosynthesis and proteolysis are both important processes involved in ovarian follicular development, which may be influenced by cytochrome P450 (CYP)-dependent fatty acid metabolites. However, CYP-dependent lipid metabolism has not been characterized with respect to follicular maturation *in vivo*. Therefore, follicular fluid was collected in the hours before and after the LH surge in pigs, and concentrations of epoxy, hydroxy, and dihydroxy lipids were measured by liquid chromatography tandem mass spectrometry. Arachidonate oxidation and epoxyeicosatrienoic acid hydrolysis to dihydroxyeicosatrienoic acids (DHETs) were also assessed in thecal and granulosa tissue fractions, and the expression of CYP epoxygenases was evaluated by immunoblots using available antisera. To evaluate soluble epoxide hydrolase (sEH) expression, the porcine sEH was cloned from ovarian tissue, expressed and purified for antibody generation. The follicular fluid oxylipin concentrations ranged from 1–150 nM depending on the compound and estrous stage. The follicular fluid concentrations of CYP-dependent oxylipins increased at estrus, as did sEH expression; however, significant changes in epoxides were not observed, and the 11,12-DHET peak was delayed. The ratio of 14,15–DHET:11,12-DHET across all samples correlated with the log of follicular fluid estradiol concentrations ($P < 0.01$). Epoxygenase activities were similar in theca and granulosa, varying little with follicular development, whereas the decline of a single CYP2J isoform at ovulation was observed by immunoblots. The sEH activity was higher in granulosa than in theca. Finally, the dynamic changes in follicular CYP-dependent arachidonic acid metabolites and their modulatory function in vascular models suggest roles for these metabolites in follicular maturation, which may include regulation of estradiol biosynthesis and preovulatory remodeling of the follicular wall that should be fully explored in future studies. (*Endocrinology* 145: 5097–5105, 2004)

---

THE CATALYTIC OXIDATION of arachidonic acid (AA) produces an array of potent bioactive compounds derived from cyclooxygenase- (COX), lipoxygenase- (LOX), and cytochrome P450 (CYP)-dependent processes. Ovulation occurs concomitant with an increase in COX and LOX metabolism (1); however, CYP-dependent AA metabolism has been poorly studied in the intact ovary. In culture, luteinized granulosa cells synthesize epoxy eicosatrienoic acid (EETs) via CYP pathways and can transform EETs into their corresponding diols (2–6). Changes in the ovulatory follicle include hyperemia, edema, and fibroblast proliferation in the surrounding theca externa (7), and many of these processes are influenced by oxylipins produced by CYP metabolism (8, 9). As a rule, EETs are vasodilators (8). 14(15)-EET has also been shown to induce vascular COX expression (10), competitively inhibit prostaglandin $E_2$ synthesis (11), and mod-

ulate estradiol synthesis *in vitro* (3). In addition, 11(12)-EET and its corresponding diol are fibrinolytic, inducing plasminogen activator expression (11a), and have antiinflammatory properties, inhibiting nuclear factor-κB-mediated signaling (8). Changes in theca interna blood flow (12, 13), COX expression (14), estradiol biosynthesis (15), and plasminogen activator expression (16) are all reported ovulatory events. Therefore, one could anticipate dynamic changes in EET production in the hours leading up to ovulation.

Little is known about EET production and degradation in the ovary during follicular maturation. Cytosolic concentrations of EETs are regulated by their rates of synthesis and degradation (17) along with sequestration and release from phospholipids (18). The synthesis of EETs is primarily catalyzed by enzymes of the CYP2 family, being dominated by 2Cs and 2Js (8). However, the relative abundance of the four regioisomeric EETs produced by each epoxygenase varies considerably (19, 20). In most tissues, the soluble epoxide hydrolase (sEH) dominates epoxy lipid degradation, mediating the formation of the corresponding vicinal- or 1,2-diols; however, metabolism by β-oxidation and ω-hydroxylation has also been reported in mammals (8). The microsomal epoxide hydrolase has also been reported to hydrolyze epoxy fatty acids, albeit at a greatly reduced rate (21). sEH is primarily localized in the cytosolic compartment (22) and is present in the ovary (10, 23); however, ovarian distribution of this enzyme has not been reported to our knowledge.

To date, *in vivo* evidence linking EETs with steroidogenesis, ovarian function, or ovulation is scant. The present experiments were designed to document CYP-dependent lipid metabolism in maturing ovarian follicles while testing the hypothesis that CYP-derived lipids are elevated in the preovulatory follicle. These results are related to follicular maturation through correlative analyses with steroid hormone levels. To complement these data, thecal and granulosa tissues were examined for the expression of sEH using polyclonal antibodies directed against recombinant porcine ovarian sEH along with available antibodies for CYP2Cs and CYP2Js. To our knowledge, this is the first study to document the levels and changes in CYP-derived oxylipins in mammalian ovarian follicular fluid and to report the tissue distribution of sEH in the ovarian follicle.

## Materials and Methods

### Animals

The tissues used for this study were collected as part of previously published work (24) from animals handled in compliance with the Guide for the Care and Use of Agricultural Animals in Agricultural Research and Teaching (25) with institutional animal care and use committee approval. The animals, method of tissue collection, steroidogenic enzyme analysis, and follicular fluid steroid concentrations were described by Corbin *et al.* (24). Briefly, litters were weaned from crossbred (Landrace × Yorkshire) sows at 16–20 d (mean ± SEM, 18.0 ± 0.3 d) of lactation, after which sows were observed for estrous activity twice daily, using a mature boar. Sows were slaughtered from 3 d after weaning through 48 h after estrus, providing ovarian follicles at varied stages of preovulatory development through to the initiation of ovulation. Follicle diameters (range, 3–9 mm) were recorded and follicular fluid estradiol (range, 2–492 pg/ml) and progesterone (12–624 pg/ml) concentrations were subsequently measured as previously reported (24). Follicles were microdissected to isolate thecal and granulosa cell layers. Sows were grouped based on a combined assessment of mean follicle diameter, follicular fluid estradiol concentration, and behavior as previously described (15, 26): preestrus (n = 3), estrus (n = 5), post-LH (n = 9), and ovulatory (n = 2; some ruptured follicles observed at collection).

### Microsome and cytosol preparation

The largest follicles on both ovaries (10–12/animal) were pooled within each animal and frozen immediately on dry ice. Cells and tissues from each pool were homogenized on ice in buffer [0.1 M potassium phosphate (pH 7.4), 20% glycerol, 5 mM β-mercaptoethanol, and 0.5 mM phenylmethylsulfonylfluoride] at a ratio of approximately 1 ml buffer/0.1 g tissue. Microsomes were enriched by subcellular fractionation as previously described (27, 28). After a brief sonication, cellular debris and mitochondria were removed by centrifugation at 15,000 × *g* for 10 min. The supernatant was centrifuged at 100,000 × *g* for 60 min, the supernatant (soluble fraction containing the cytosol) was recovered, the pellet (microsomal fraction) was resuspended in homogenization buffer containing 1 mM (3-[3-cholamidopropyl-dimethylammonio]-1-propanesulfonate), and both were stored frozen. Protein concentrations of microsomal and cytosolic fractions were determined using the bicinchoninic acid protein assay (Pierce Chemical Co., Rockford, IL). The purity of microsomal fractions has been demonstrated previously by immunoblot analysis for microsomal and mitochondrial proteins (28).

### RNA isolation, cloning, and expression

Porcine ovarian mRNA was isolated from preovulatory tissues and reverse transcribed into cDNA using SuperScript reverse transcriptase (Invitrogen Life Technologies, Carlsbad, CA). Degenerate primers, designed to conserved regions of human, mouse, and rat sEH C-terminal catalytic sites, (5′-GTNTTYATNGGNCAYGAYTGG-3′ and 5′-CNAC-NCCNGGYTCYTGRAA-3′) were used to amplify a fragment of porcine sEH employing the following conditions: 35 cycles of 94 C for 45 sec, 55

C for 1 min, and 72 C for 1 min. The pig sEH fragment generated (190 bp) was cloned into pBluescript and sequenced (DNA Sequencing Facility, University of California-Davis). New primers were designed for rapid amplification of cDNA 5′-ends (Invitrogen Life Technologies) and rapid amplification of cDNA 3′-ends (Takara, Madison, WI) to determine the sequence of the entire porcine sEH cDNA. Based on this sequence, PCR primers were then designed to the N and C termini of the porcine sEH to isolate the full-length cDNA (GenBank accession no. AY566232), which was ligated into pCR2.1. The resulting full-length porcine sEH cDNA clone was excised from the pCR2.1 using *Eco*RI and ligated into pACUW21 baculovirus expression vector (pACUW21-psEH). The recombinant baculovirus was then generated, and porcine sEH protein was overexpressed as previously described (29). Porcine sEH was purified from the cell lysate by affinity chromatography (30). Protein concentration was quantified using the Pierce bicinchoninic acid assay (Pierce Chemical Co.), using fraction V BSA as the calibration standard. Epoxide hydrolase activity was measured using racemic [³H]*trans*-1,3-diphenylpropene oxide ([³H]tDPPO) (31). The preparation was judged to be pure by SDS-PAGE stained with Coomassie Brilliant Blue. Polyclonal antibodies were raised against recombinant porcine sEH in male New Zealand White rabbits (Animal Resources Service, University of California-Davis). Four weeks after the initial injection (100 μg porcine sEH), the animals were boosted every 2 wk until no additional increase in antibody titer was observed. Titer was analyzed by ELISA and Western immunoblot using the recombinant protein.

### Western blot analysis

Microsomal (10 μg) and cytosolic (20 μg) proteins were separated by electrophoresis on 8% SDS-PAGE in electrode buffer (50 mM Tris, 383 mM glycine, 0.1% sodium dodecyl sulfate, and 0.4 mM EDTA). Separated proteins were transferred onto polyvinylidene difluoride membranes (Immobilon P, Millipore Corp., Bedford, MA) and detected with polyclonal antibody raised against recombinant proteins. Antibodies were obtained from various sources: CYP2J courtesy of Dr. Darryl Zeldin (NIEHS, Research Triangle Park, NC), CYP2C8 and CYP2C9 from Gen-Test (Woburn, MA), and sEH produced as described. Immunoblotting procedures were carried out at room temperature in PBS with 0.1% Tween 20 (Amresco, Solon, OH). After blocking in 10% dried milk, the proteins were visualized by incubating the membranes with donkey antirabbit horseradish peroxidase-linked IgG whole antibody (Amersham Biosciences, Arlington Heights, IL) at a 1:10,000 dilution, washing, then generating a chemiluminescent signal using Luminol reagent (NEN Life Science Products, Boston, MA) detected by autoradiography.

### Follicular fluid lipid extraction

Follicular fluid aliquots (50–100 μl) were thawed, spiked with analytical surrogates (~1 pmol/sample), and extracted using modifications of published procedures (32). Briefly, samples were extracted three times with 100 μl ethyl acetate, the organic phases were combined, and solvent was removed under dry nitrogen. The resulting residue was spiked with internal standards, redissolved in 50 μl methanol, and stored at −20 C until analysis.

### Tissue oxylipin metabolic capacity

The biochemical activities of a series of polyunsaturated fatty acid oxidases and epoxide hydrolases were determined in microsomal and cytosolic (soluble) fractions of both granulosa and thecal cells. Fatty acid epoxygenase, ω-hydroxylase, midchain hydroxylase, and prostaglandin synthase activities were obtained simultaneously. Briefly, duplicate aliquots (~50 μg) were suspended in 100 μl 0.1 M sodium phosphate buffer (pH 7.4) and were incubated (60 min, 30 C) with arachidonic acid (100 μM) in the presence of an NADPH-regenerating system. Reactions were halted with the addition of 100 μl methanol and centrifuged to remove the protein precipitate. Incubations were then spiked with analytical surrogates, and arachidonate oxidation products were quantified in the isolated supernatant using the lipid chromatography/mass spectrometry/mass spectrometry method described below. sEH activity was determined using tDPPO as the substrate (31). Briefly, 1 μl tDPPO in dimethyl formamide was added to 100 μl tissue homogenate in sodium phosphate buffer (0.1 M; pH 7.4) containing 0.1 mg/ml BSA (final tDPPO

concentration, 50 $\mu$M) and incubated for 30 min at 30 C. The reactions were quenched by the addition of 60 $\mu$l methanol and 200 $\mu$l isooctane, followed by vortexing. The diol metabolites were quantified by liquid scintillation counting of the aqueous phase. Assays were performed in triplicate. Controls for background glutathione transferase activity were performed (33) and were subtracted when necessary. Counts per minute were converted to picomoles of product and averaged for triplicate determinations. Specific activities were expressed as picomoles per minute per milligram of protein.

### Oxylipins analysis

Oxidized lipids were measured in tissue and assay extracts using negative mode electrospray ionization with a tandem quadrupole mass spectral detector (Quattro Ultima, Micromass, Manchester, UK) operated in multireaction monitoring mode. Follicular fluids were assayed using slight modifications of previously described methods for CYP-dependent metabolite quantification (32, 34). Modifications of HPLC (Table 1) and mass spectral acquisition parameters (Table 2) allowed detection and quantification of the reported epoxygenase-, lipoxygenase- (*i.e.* midchain hydroxylation), and cyclooxygenase-dependent metabolites.

### Chemical nomenclature

Following the recommendations of Smith *et al.* (35, 36), epoxy fatty acid abbreviations indicate epoxide position, chain length, and degrees of unsaturation. Therefore, 14(15)-epoxyeicostri-(5Z,8Z,11Z)-enoic acid is reduced to 14(15)-EpETrE, whereas 9(10)-epoxyoctadec-(12Z)-enoic acid becomes 9(10)-EpOME. Dihydroxy lipids are named similarly, such that 14,15-dihydroxyeicostri-(5Z,8Z,11Z)-enoic acid becomes 14,15-Di-HETrE, and 20-hydroxyeicosatetra-(5Z,8Z,11Z,14Z)-enoic acid is 20-HETE. The EpETrEs and DiHETrEs are more commonly known as EETs and DHETs, respectively, and these common abbreviations are used to improve manuscript readability. Additionally, cyclooxygenase-dependent metabolites are abbreviated as follows: prostaglandin $E_2$ as $PGE_2$; and the stable metabolite of prostacyclin, 6-keto-prostaglandin $F_{1\alpha}$ as 6-keto-$PGF_{1\alpha}$.

### Statistical analysis

Differences among tissues isolated from follicles at different stages of development were evaluated by one-way ANOVA. A paired *t* test was used to evaluate differences between thecal and granulosa sEH activity. A one-tailed *t* test, assuming unequal variance, was used to evaluate differences in oxylipin concentrations and compositions. The potential for type I errors resulting from the multiple ANOVAs performed was controlled using a sequentially rejective method for multiple comparison adjustment. This approach compares calculated, ranked *P* values with modified levels of significance ($\alpha^* = \alpha/n$, where n = the number of statistical comparisons and $\alpha = 0.05$); significance was determined when $P \leq \alpha^*$. Associations between oxylipin concentrations or ratios and follicular fluid estradiol concentrations were calculated after log transformation of the steroid values.

**TABLE 1.** HPLC parameters

| Time (min) | % A | % B |
|---|---|---|
| 0.00 | 85.0 | 15.0 |
| 0.50 | 85.0 | 15.0 |
| 2.00 | 70.0 | 30.0 |
| 8.00 | 45.0 | 55.0 |
| 28.00 | 25.0 | 75.0 |
| 29.00 | 0.0 | 100.0 |
| 33.00 | 0.0 | 100.0 |
| 33.10 | 85.0 | 15.0 |
| 35.00 | 85.0 | 15.0 |

Solution A, Water/0.1% acetic acid (wt/wt); solution B, 80:15 (v/v) acetonitrile/methanol/0.1% acetic acid (wt/wt); flow rate, 350 $\mu$l/min; column, 2.1 × 150 mm, 5-$\mu$m $C_{18}$(2) Luna (Phenomenex, Torrance, CA).

**TABLE 2.** Electrospray ionization tandem mass spectroscopy parameters

| Analyte | $t_R$ (min) | Mass transition (Da) | Collision voltage (V) |
|---|---|---|---|
| 6-Keto-$PGF_{1\alpha}$ | 7.2 | 369.2 > 163.1 | 24 |
| $PGE_2$ | 9.1 | 351.2 > 271.2 | 14 |
| 12,13-DHOME | 13.6 | 313.2 > 183.1 | 23 |
| 9,10-DHOME | 14.1 | 313.2 > 201.1 | 23 |
| 14,15-DHET | 14.7 | 337.2 > 207.1 | 17 |
| 11,12-DHET | 15.6 | 337.2 > 167.1 | 20 |
| 8,9-DHET | 16.4 | 337.2 > 127.1 | 20 |
| 20-HETE | 17.2 | 319.2 > 275.2 | 16 |
| 5,6-DHET | 17.5 | 337.2 > 145.1 | 17 |
| 15-HETE | 19.7 | 319.2 > 219.1 | 13 |
| 11-HETE | 20.5 | 319.2 > 167.1 | 14 |
| 12-HETE | 21.1 | 319.2 > 179.1 | 14 |
| 5-HETE | 22.3 | 319.2 > 115.1 | 14 |
| 12(13)-EpOME | 23.1 | 295.2 > 195.1 | 17 |
| 14(15)-EET | 23.4 | 319.2 > 219.1 | 13 |
| 9(10)-EpOME | 23.6 | 295.2 > 171.1 | 17 |
| 11(12)-EET | 24.8 | 319.2 > 208.1 | 13 |
| 8(9)-EET | 25.2 | 319.2 > 155.1 | 13 |
| 5(6)-EET | 25.7 | 319.2 > 191.1 | 10 |

Cone voltages of 55 V (epoxides and HETEs) and 60 V (prostanoids and diols) were used for these analyses. Collision-induced dissociation was performed with argon at a pressures of 2.3 mTorr.

## Results

### Classification of follicular development

The classification of the stage of follicular development (preestrus, estrus, and post-LH) was based on sexual behavior and follicle diameters that correlated with changes in estradiol, progesterone, and LH, as reported previously (15, 27). In the current study the preestrous group had relatively low estradiol and progesterone levels (27.5 ± 13.5 and 73.3 ± 32.2 ng/ml, respectively) compared with the estrous group that had high estradiol and high progesterone levels (266.8 ± 70.4 and 347.8 ± 85.3 ng/ml, respectively) and the post-LH group that had low estradiol and high progesterone levels (7.7 ± 2.4 and 403.2 ± 134.4 ng/ml, respectively). Follicles collected from the two additional animals found to be in the process of ovulation contained very low concentrations of estradiol (3.6 and 1.3 ng/ml) and extremely high concentrations of progesterone (2915 and 4881 ng/ml), even compared with animals in the post-LH group.

### Follicular fluid oxylipins

The cytochrome P450-derived polyunsaturated fatty acids were readily detected in the follicular fluid samples described above at concentrations up to 150 nM (Fig. 1). Both arachidonate and linoleate metabolites were identified, and the sum of all arachidonate products was within 1 order of magnitude of the total of linoleate products measured. Epoxides, diols, and 20-HETE were detected in each sample (Figs. 1 and 2), consistent with the expression of epoxygenase, epoxide hydrolase, and $\omega$-hydroxylase enzymes in follicular tissues. Three of the four EET regio-isomers were detected in six of 18 samples. 8(9)-EET was not observed in all groups, and it must be noted that 5(6)-EET recoveries with the applied method are approximately 25% (32). We have since confirmed our earlier supposition that losses are due to
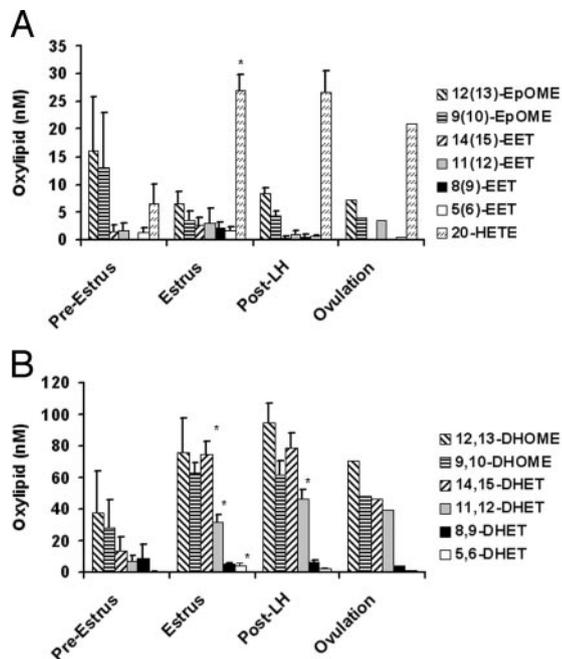
FIG. 1. Concentrations of CYP-dependent linoleate and arachidonate metabolites detected in ovarian follicle fluids. The metabolites produced by CYP metabolism, including epoxides and the ω-hydroxy arachidonate (20-HETE), are shown in A. The measured dihydroxy fatty acids are shown in B. The concentrations of 20-HETE and all detected diols increased from preestrus to estrus, and generally remained elevated through ovulation. However, the rates of increase and decline appeared to vary among components. The arachidonate epoxides (EETs) were observed intermittently at levels near the detection limit of 1 nM, whereas the linoleate epoxides (EpOMEs), linoleate diols (DHOMEs), arachidonate diols (DHETs), and 20-HETE were routinely observed. Results are the mean ± SE (n = 3, 5, and 9, respectively) for preestrus, estrus, and post-LH and the mean for ovulation (n = 2). *, Concentrations significantly different from those found in the previous stage ($P < 0.05$).
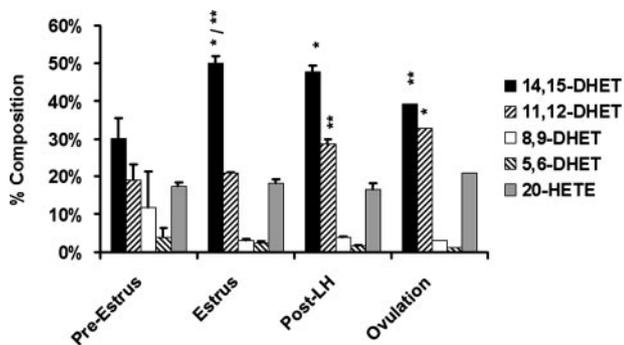


FIG. 2. Follicular fluid DHET and 20-HETE expressed as a percentage of the total measured CYP-dependent lipid metabolites. The relative abundance of 20-HETE remained constant, whereas that of the arachidonate diols, in particular, 14,15-DHET and 11,12-DHET, changed dramatically. Results are the mean ± SE (n = 3, 5, and 9, respectively) for preestrus, estrus, and post-LH and the mean for ovulation (n = 2). *, Compositions significantly different from those in preestrus; **, compositions different from those in the previous stage ($P < 0.05$).

5(6)-δ lactone formation, and not 5,6-DHET formation (unpublished observations).

When expressed as a percentage of the total CYP-derived oxylipins (Fig. 2), the detected 20-HETE was quite stable

(20 ± 6%) across all follicle classes. The relative abundance of epoxide regio-isomers were 14(15)>11(12)>5 (6)-[42 (± 21):24 (± 26):3 (± 2)] for the EETs and 12(13)>9 (10)-[67 (± 6):33 (± 6)] for the EpOMEs. The high variability of the EET isomeric ratios was probably due to the low magnitude (<5 nM) of these residues. The relative abundance of the diol regio-isomers generally tracked those observed for epoxides with 14,15>11,12->≫ 8,9-~5,6-[58 (± 7):34 (± 6):5 (± 2):3 (± 3)] for the DHETs, and 12(13)->9(10)-[57 (± 7):43 (± 7)] for the dihydroxy octadeceneoic acids.

In follicular fluid, the concentrations of epoxides (Fig. 1A) were routinely less than those of diols (Fig. 1B) in all groups. When the sum of all epoxides and diols was evaluated, the epoxide:diol ratio was higher ($P < 0.05$) in samples from the preestrous group (mean, 0.45) compared with all other stages (mean, 0.06–0.07). At estrus, the concentrations of 20-HETE and 14,15-, 11,12-, and 5,6-DHET increased approximately 5-fold, whereas epoxide levels remained constant. 11,12-DHET continued to increase into the post-LH period. The relative abundance of the diols and 20-HETE within each group was then calculated (Fig. 2). These data treatment greatly reduced the variability and allowed visualization of clear trends. At estrus, 14,15-DHET increased from 30% to 50% of the total measured CYP metabolites; this held through the post-LH period and declined at ovulation to a level indistinguishable from the preestrous value. In contrast, the relative abundance of 11,12-DHET was unchanged between preestrus and estrus, but was elevated between estrus and post-LH, and it was significantly different from the preestrous ratios at ovulation. When expressed as a ratio, 14,15-DHET:11,12-DHET was highest in the estrous follicular fluid samples, whereas no change was seen with linoleate-derived diols (Fig. 3A). In addition, although the magnitude was low (1–5 nM), concentrations of 5,6-DHET also showed a phased distribution, with peak concentrations at estrus (Fig. 3B). The relationship between steroid and oxylipin concentrations was complex, and direct correlations were not observed between steroids and oxylipin concentrations. This was in part because steroid levels varied markedly, more than 2 orders of magnitude in the case of estradiol. However, after natural log transformation of the raw estradiol concentrations (Ln $E_2$), correlations were evident between this and certain lipids (Fig. 3C). Specifically, Ln $E_2$ was correlated with the ratio of 14,15-DHET:11,12-DHET ($y = 0.24x + 1.16$; $r^2 = 0.80$; n = 18; $P < 0.01$) with all individuals included. In addition, Ln $E_2$ correlated with 5,6-DHET concentrations among samples of the post-LH group, including those from the two ovulating animals ($y = 1.02x + 0.64$; $r^2 = 0.86$; n = 11; $P < 0.01$). After eliminating two outlying 5,6-DHET levels, the pre-LH 5,6-DHET concentrations also showed a strong correlation with Ln $E_2$ ($y = 0.46x - 0.07$; $r^2 = 0.89$; n = 6; $P < 0.05$), which was distinct from the post-LH regression. No correlations with progesterone were observed.

### In vitro oxylipin metabolism

AA metabolism by thecal and granulosa microsomes was assayed to document oxylipin synthase activity, whereas sEH activity was measured in soluble fractions. Samples from each of the study animals were not available for these
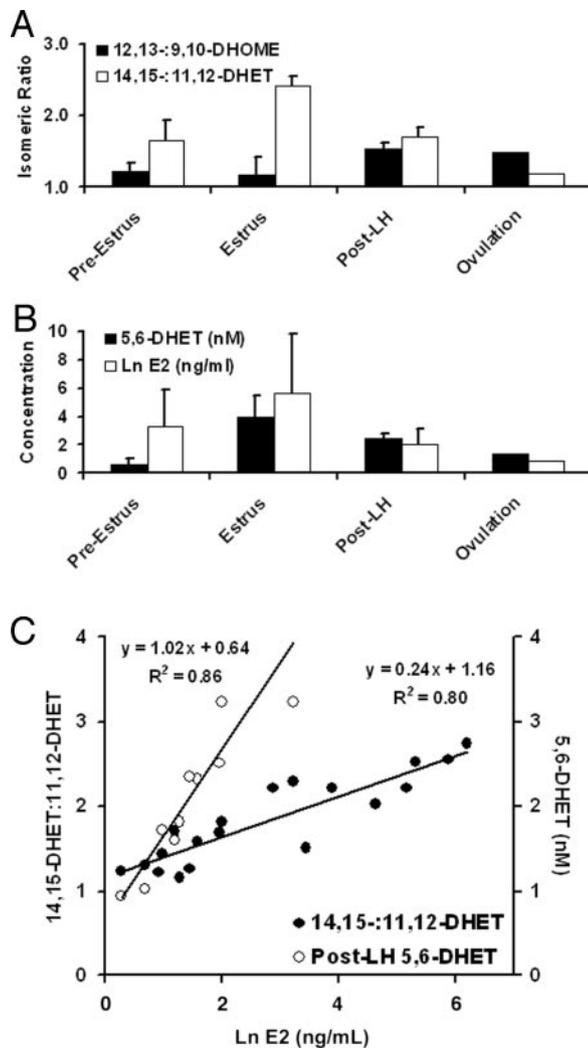
FIG. 3. Specific oxylipins derived from P450-epoxygenase metabolism showed complex associations with follicular fluid estradiol concentrations. In particular, the ratio of 14,15-DHET to 11,12-DHET showed a clear shift during the ovulatory cycle, with the 14,15-isomer reaching an apex at estrus (A). Similar changes in the linoleate diols were not observed. Although of low magnitude, the concentrations of the 5,6-DHET isomer also reached a maximum at estrus, as did those of estradiol (B). The changes in the 14,15-:11,12-DHET ratio correlated strongly with the natural log of the estradiol concentration (Ln E2), as did the post-LH 5,6-DHET concentration ($P < 0.01$; C). With the exclusion of two points (preestrous 5,6-DHET, 0; estrous 5,6-DHET, 9.7), the pre-LH 5,6-DHET concentration showed an independent correlation with Ln E2 ($y = 0.46x - 0.07$; $r^2 = 8.9$; n = 6; $P < 0.05$). The concentrations of other measured oxylipins did not show similar trends. The results in A and B are the mean $\pm$ SE (n = 3, 5, and 9, respectively) for preestrus, estrus, and post-LH and the mean for ovulation (n = 2).

assays, and the acquired sets were too small to represent all corresponding groups. Thus, preestrous and estrous data were combined to represent pre-LH values for comparison with post-LH values only. Microsomal epoxygenase activity (Table 3) was indicated in both compartments of the follicle by 14,15- and 11,12-DHET synthesis, at similar levels in each and without marked differences between the pre-LH and post-LH specimens. The appearance of DHETs in these incubations is consistent with the presence of sEH in these

microsomal preparations as previously reported (37–39). Synthesis of 20-HETE was not observed, but 15-, 12-, 11-, and 5-HETE were formed in both thecal and granulosa tissues. Activities ranged from 0.10–5.6 pmol/min·mg microsomal protein of the individual samples, with 15-HETE and 5-HETE being the most abundant isolated metabolites. The production of 6-keto-PGF$_{1\alpha}$ was exclusively by the theca and increased 6-fold during the post-LH period ($P < 0.01$). In contrast, PGE$_2$ synthesis was readily detectable in both thecal and granulosa microsomal incubations. Although granulosa synthesis of PGE$_2$ appeared to increase during the post-LH period, it did not reach statistical significance with the number of samples analyzed ($P > 0.05$).

*Ovarian epoxygenases*

Several candidate CYP epoxygenases were detectable by immunoblot analysis in porcine liver microsomes using antibodies to human CYP2C8, CYP2C9, and CYP2J (data not shown), but only CYP2J was detected in follicular tissues (Fig. 4). Although three definitive bands were evident in immunoblots for CYP2J in liver microsomes, only one band was seen in thecal and granulosa microsomes, corresponding in size to the middle band of the hepatic triplet. CYP2J expression was higher in theca than in granulosa and was lost as follicles matured, appearing to decrease in both compartments.

*Ovarian sEH*

A preliminary evaluation of the cross-reactivity of available sEH antibodies with porcine tissues indicated weak or nonspecific interactions. Therefore, efforts were made to clone and express the porcine sEH from ovarian tissues. The sequence of the isolated porcine sEH gene (GenBank accession no. AY566232) had an 82% identity to the human ortholog. The predicted molecular mass of this gene product is 62.8 kDa, and an apparent molecular mass of approximately 60 kDa was found for the expressed and purified protein using SDS-PAGE. The specific activity based on tDPPO diol formation by the recombinant enzyme was $10.7 \pm 0.1$ μmol/min·mg, which is comparable to other mammalian sEHs (40). Antibodies (1:5000 dilution) against this protein (antibody 468) were evaluated for cross-reactivity with available recombinant sEHs (10 μg/well), including those from mouse, rat, human, cress, and potato. The pig sEH antibody also detected the rat and mouse enzyme, although with lower sensitivity than observed for the pig enzyme. This antibody produced very faint bands with human sEH, whereas plant enzymes were not detected (data not shown).

Using the porcine sEH antibodies for immunoblot analysis indicated that the sEH protein level was lower in tissues from follicles harvested in the post-LH period (Fig. 4). Although sEH activity appeared to decrease in both theca and granulosa in the post-LH period, too few samples were available for a valid statistical analysis by group. However, the sEH activity was consistently higher in the granulosa than in the theca in pairwise comparisons within individual pigs (mean difference, $0.49 \pm 0.14$ nmol/min·mg; $P < 0.01$; n = 10) and was correlated positively between the two follicular tissue compartments ($r^2 = 0.65$; $P < 0.05$).

**TABLE 3.** Porcine preovulatory follicle thecal and granulosa cell microsome AA metabolite production (picomoles per minute per milligram of protein)

| | Theca[a] | | | | Granulosa[a] | | | |
|---|---|---|---|---|---|---|---|---|
| | Pre-LH[b] | n[c] | Post LH | n[c] | Pre-LH[b] | n[c] | Post-LH | n[c] |
| 14,15-DHET | 0.45 ± 0.07 | 7 | 0.30 ± 0.07 | 7 | 0.42 ± 0.13 | 4 | 0.38 ± 0.06 | 6 |
| 11,12-DHET | 0.33 ± 0.05 | 7 | 0.22 ± 0.05 | 7 | 0.32 ± 0.12 | 4 | 0.35 ± 0.10 | 6 |
| 15-HETE | 2.37 ± 0.51 | 7 | 2.56 ± 0.60 | 7 | 2.89 ± 0.93 | 4 | 4.15 ± 1.20 | 6 |
| 11-HETE | 0.75 ± 0.14 | 7 | 0.86 ± 0.19 | 7 | 1.04 ± 0.44 | 4 | 1.27 ± 0.31 | 6 |
| 12-HETE | 1.16 ± 0.25 | 5 | 0.80 ± 0.19 | 4 | 0.76 ± 0.12 | 3 | 1.13 ± 0.28 | 4 |
| 5-HETE | 1.90 ± 0.37 | 7 | 1.95 ± 0.40 | 7 | 2.81 ± 1.29 | 4 | 3.15 ± 0.82 | 6 |
| 6-Keto-PGF$_{1\alpha}$ | 0.14 ± 0.11 | 7 | 0.87 ± 0.22 | 6 | 0.04 ± 0.05 | 4 | 0.05 ± 0.05 | 6 |
| PGE$_2$ | 0.12 ± 0.04 | 7 | 0.32 ± 0.16 | 7 | 0.17 ± 0.10 | 4 | 0.92 ± 0.52 | 6 |

[a] Thecal and granulosa microsomes protein (~50 µg/reaction) from individual pigs were incubated with AA (100 µM), and oxidation products were quantified by liquid chromatography/mass spectrometry/mass spectrometry (see *Materials and Methods*). Results are the mean ± SE of triplicate incubations.

[b] Due to limited sample availability, data from preestrous and estrous groups were combined for this analysis and are represented as the pre-LH values for comparison with those from the post-LH group.
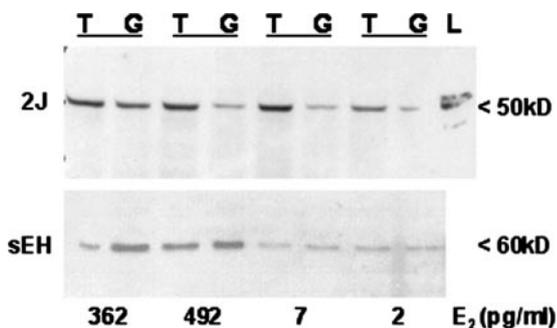
[c] Number of observations.



FIG. 4. Western immunoblot analysis of porcine ovarian theca (T) and granulosa (G) for expression of cytochrome P450 2J (2J; *upper panel*) and sEH (*lower panel*). Microsomal protein (10 µg) for 2J and cytosolic protein (20 µg) for sEH were isolated from thecal and granulosa tissues of preovulatory follicles, separated by gel electrophoresis, and immunoblotted (details in *Materials and Methods*). The estradiol concentrations (picograms per milliliter) measured in fluid from the same follicles are shown below the corresponding lanes. The molecular sizes of the immunodetected bands are shown (*right*), and liver (L; 10 µg; *upper panel*) was included as a positive control for 2J expression. Immunodetectable bands were observed in the liver, but not in the ovary, using anti-CYP2C8 and anti-CYP4A antibodies (data not shown).

## Discussion

Maturation of the ovarian follicle is associated with dynamic and carefully orchestrated changes in both physical structure and biochemical activity of thecal and granulosa cells. Although the complete nature of this regulation is still poorly understood, lipid oxidation products are likely to play a critical role. The goal of this study was to evaluate changes in endogenous oxylipin concentrations and potential sites of arachidonic acid metabolism in the maturing follicle, focusing primarily on CYP-dependent processes. Although highlighting CYP-dependent metabolites, COX- and LOX-dependent metabolism was also investigated, allowing a certain degree of consistency and comparability of current results with previously published findings. For instance, an apparent increase in granulosa PGE$_2$ synthesis was observed in the post-LH period consistent with COX induction by LH (41) and the importance of PGE$_2$ in the ovulatory process (42, 43). In addition, prostacyclin synthesis (based on 6-keto-PGF$_{1\alpha}$ production) was restricted to the theca and increased in the post-LH period, findings consistent with previous reports (44–46). Therefore, these findings with COX metabolism indicate that thecal and granulosa tissue isolates were pure, and the applied biochemical and analytical evaluations appear valid.

Consistent with previous studies (2–4, 6), we confirmed the ability of follicular tissue to synthesize epoxy and dihydroxy fatty acids, but also report the presence of ω-hydroxylation products in follicular fluid. Dynamic changes in follicular fluid CYP-dependent fatty acid metabolites were observed during the preovulatory period examined. Although the concentration of epoxides in follicular fluid was constant, in the low nanomolar concentration range, linoleate and arachidonate diols as well as 20-HETE levels generally increased at estrus and remained elevated through ovulation. Therefore, it would appear that the flux of fatty acids through CYP-dependent metabolism increases approximately 5-fold at estrus. The increase in diol formation was coincident with elevated sEH levels, which also appeared positively correlated with follicular fluid estradiol concentrations. In addition, the expression of sEH in both thecal and granulosa cells along with its post-LH decline are reminiscent of the tissue-specific and temporal regulation of porcine gonadal P450 aromatase (15), the key enzyme metabolizing androgens to estrogens. It is interesting to note that both sEH (47) and the dominant CYP ω-hydroxylases (48) are induced by androgens, and the declining androgen production in the follicle may be functionally related to the decrease in sEH expression. The failure of sEH-dependent metabolites to decline in follicular fluid along with the drop in sEH expression suggest that these compounds may be selectively retained in this compartment, unlike the steroid hormones.

The functional consequences of the altered oxylipin concentrations are unclear at present; however, the close association with estrus argues for an influence on estradiol synthesis. In fact, in human luteinized granulosa cell cultures, 14(15)-EET was shown to increase estradiol production at 1–5 nM while inhibiting it at 10–50 µM (3). In the present study, concentrations of the sum of 14(15)-EET and DHET in follicular fluid were in the low nanomolar range, suggesting the potential for a stimulatory effect on estradiol synthesis *in vivo*. A direct stimulatory effect of this or other epoxide

isomers on estradiol biosynthesis would predict a positive correlation between the concentration of the causal factor and the responsive agent. In fact, no such relationship was found between any of the observed follicular fluid oxylipins and estradiol. However, the relative abundance of 14,15-DHET and 11,12-DHET showed a strong positive correlation with follicular estradiol concentrations, reaching a maximum of 14,15-DHET over 11,12-DHET when estradiol concentrations peaked and collapsing to a 1:1 ratio at ovulation. These data suggest that the levels of specific epoxygenases may have changed differentially, and that follicular estradiol biosynthesis and arachidonate epoxidation may be mechanistically linked, as previously proposed (3). Although the influence of 11,12-DHET on estradiol synthesis has not been reported, these findings suggest that future studies be conducted to determine whether 11(12)-EET or 11,12-DHET alters estradiol synthesis, as reported for 14(15)-EET.

Other roles for CYP-generated metabolites in the maturing ovary, besides the potential modulation of steroidogenesis, are also likely. The recent finding that EETs, particularly 11(12)-EET and 11,12-DHET, enhance tissue plasminogen activator (tPA) gene expression is particularly relevant to follicular maturation (49). tPA has been implicated in the process of ovarian follicle rupture (16) and may be a critical factor in oocyte maturation (50). In fact, the abundance of tPA mRNA and protein was low in both granulosa and thecal/interstitial cells during early follicular development, but increased thereafter, reaching the highest levels in the preovulatory period (51). These reports parallel our current finding of increasing levels of 11,12-DHET in the follicular fluid of the maturing ovary and implicate 11(12)-EET as a potential regulator of the follicular wall remodeling that occurs before ovulation (51). In addition, the EETs are endothelial-derived hyperpolarizing factors (8) that may act in concert with prostacyclin to regulate thecal blood flow.

As alluded to above, one means of regulating the isomeric ratios of oxylipins would be to alter the relative abundance or activity of different epoxygenases with unique isomeric product ratios. For instance, CYP2C8 activity is consistent with the tissue concentrations and chirality of EETs in human liver, where values of 14(15)-EET exceed those of 11(12)- and 8(9)-EETs (52). In contrast, CYP2C3 in rat kidney cortex may be responsible for the elevation of 11(12)-EET over both 8(9)- and 14(15)-EETs (53). Renal microsomes from spontaneously hypertensive rats also exhibit increased 14(15)- and 11(12)-EET synthesis over normotensive wild-type rats in association with the increase in expression of a CYP2J isoform (54), which, as a family, favor 14,15-epoxidation (55). A similar profile seems to exist in the porcine ovarian follicle.

To test the hypothesis that differences in CYP-dependent oxylipin profiles reflected tissue-specific expression of CYPs with differing regio- and stereo-selectivity for substrate oxidation, microsomal fractions were incubated with AA and an NADPH-regenerating system. Although thecal preparations produced more 14,15- products than 11,12- products in both pre- and post-LH groups, the post-LH, but not pre-LH, granulosa cell preparations showed a 14,15-:11,12-DHET product ratio of 1:1, suggesting that granulosa CYPs may be responsible for the observed changes in follicular fluid arachidonate products.

The failure to find differences in AA metabolite production between pre- and post-LH thecal and granulosa microsomes was not consistent with the changing metabolite profiles in follicular fluid. However, follicular fluid steroid concentrations differed between animals in the preestrous and estrous groups, which were combined for logistic reasons in these analyses. Given the relationship between estradiol concentration and follicular fluid diols, these data can only be interpreted as evidence of the presence of enzyme activity, not the absence of changes with follicle maturation in either tissue compartment, which require more extensive study. Western blots detected a single CYP2J isoform in the maturing ovary, which comigrated with a CYP2J isoform from human granulosa cells (data not shown), and one of three isoforms was expressed in pig liver. Human liver and heart also express three CYP2Js (56). However, rather than peaking at estrus, the ovarian CYP2J protein declined progressively, with the lowest levels observed in the post-LH period. In addition, no change in total epoxygenase activity could be detected in these tissues, suggesting that the observed CYP2J may not be a critical isoform responsible for EET biosynthesis in the maturing ovarian follicle. Attempts to identify other epoxygenases by Western blot (*i.e.* CYP2C8 and 2C9) were successful in the liver, but not in the ovary, of these pigs. In addition, although 20-HETE was routinely detected in follicular fluids, 20-HETE synthesis was not detected *in vitro*. Western blots for CYP4A, the dominant AA hydroxylase enzymes, revealed detectable protein in the liver, but not ovary (data not shown).

The failure to detect 20-HETE in microsomal incubations may have been due to a lack of sensitivity for this analyte using current methods (32), where limited tissue mass was available for incubations. It is also possible that the single buffer system that was used for all microsomal P450 activities may not be optimal for some (57). The expression of any of these enzymes may have been below the limits of detection in follicular tissues, but still sufficient to contribute meaningfully to AA metabolism. Therefore, despite shifts in ratios of eicosanoid regio-isomers suggesting changes in the relative levels of specific epoxygenases in the final stages of follicle maturation, the identity of putative CYPs remains unknown. Additional studies are required to detect and define the epoxygenases most relevant to eicosanoid synthesis in follicular tissues. Whatever their identities, however, the enzymes expressed in the preovulatory follicle appear to exhibit a preference for epoxidation at double bonds distal to the carboxyl terminal of both arachidonate and linoleate.

In summary, the role of COX- and LOX-derived eicosanoids in follicular maturation and ovulation is well recognized, but little is known about the role of the epoxygenase arm of the AA cascade in these events. The present study used isolated theca and granulosa from porcine follicles to investigate epoxy eicosanoid synthesis near the time of ovulation. Oxylipin profiling of follicular fluids together with activity and immunoblot analyses identified epoxygenase synthesis and metabolic pathways in preovulatory theca and granulosa. Ratios of regio-isomers changed in concert with follicular fluid estradiol concentrations, suggesting differential regulation of specific epoxygenases during follicular maturation. At the concentrations observed, these agents may

play important roles in follicular maturation, including the regulation of estradiol biosynthesis and matrix degradation necessary for the remodeling of the follicular wall before ovulation. These events and their interactions warrant investigation in future research.

## Acknowledgments

## References

1. **Murdoch WJ, Hansen TR, McPherson LA** 1993 A review: role of eicosanoids in vertebrate ovulation. Prostaglandins 46:85–115
2. **Zosmer A, Elder MG, Sullivan MH** 1990 Production of intracellular arachidonic acid metabolites by human granulosa cells. Prostaglandins Leukotriene Essent Fatty Acids 41:265–267
3. **Van Voorhis BJ, Dunn MS, Falck JR, Bhatt RK, VanRollins M, Snyder GD** 1993 Metabolism of arachidonic acid to epoxyeicosatrienoic acids by human granulosa cells may mediate steroidogenesis. J Clin Endocrinol Metab 76:1555–1559
4. **Zosmer A, Rendell NB, Taylor GW, Elder MG, Sullivan MH** 1995 Formation and metabolism of 14,15-epoxyeicosatrienoic acid by human reproductive tissues. Biochim Biophys Acta 1258:234–240
5. **Zosmer A, Elder MG, Sullivan MH** 2003 The regulation of arachidonic acid metabolism in human first trimester trophoblast by cyclic AMP. Prostaglandins Other Lipid Mediat 71:43–53
6. **Zosmer A, Elder MG, Sullivan MH** 2002 The production of progesterone and 5,6-epoxyeicosatrienoic acid by human granulosa cells. J Steroid Biochem Mol Biol 81:369–376
7. **Espey LL, Lipner H** 1994 Ovulation. In: Knobil E, Neill J, eds. The physiology of reproduction. New York: Raven Press; 725–780
8. **Spector AA, Fang X, Snyder GD, Weintraub NL** 2004 Epoxyeicosatrienoic acids (EETs): metabolism and biochemical function. Prog Lipid Res 43:55–90
9. **Roman RJ** 2002 P-450 metabolites of arachidonic acid in the control of cardiovascular function. Physiol Rev 82:131–185
10. **Peri KG, Varma DR, Chemtob S** 1997 Stimulation of prostaglandin G/H synthase-2 expression by arachidonic acid monooxygenase product, 14,15-epoxyeicosatrienoic acid. FEBS Lett 416:269–272
11. **Fang X, Moore SA, Stoll LL, Rich G, Kaduce TL, Weintraub NL, Spector AA** 1998 14,15-Epoxyeicosatrienoic acid inhibits prostaglandin $E_2$ production in vascular smooth muscle cells. Am J Physiol 275:H2113–H2121
11a. **Node K, Ruan XL, Dai J, Yang SX, Graham L, Zeldin DC, Liao JK** 2001 Activation of G$\alpha$s mediates induction of tissue-type plasminogen activator gene transcription by epoxyeicosatrienoic acids. J Biol Chem 276:15983–15989
12. **Brannstrom M, Zackrisson U, Hagstrom HG, Josefsson B, Hellberg P, Granberg S, Collins WP, Bourne T** 1998 Preovulatory changes of blood flow in different regions of the human follicle. Fertil Steril 69:435–442
13. **Acosta TJ, Hayashi KG, Ohtani M, Miyamoto A** 2003 Local changes in blood flow within the preovulatory follicle wall and early corpus luteum in cows. Reproduction 125:759–767
14. **Joyce IM, Pendola FL, O'Brien M, Eppig JJ** 2001 Regulation of prostaglandin-endoperoxide synthase 2 messenger ribonucleic acid expression in mouse granulosa cells during ovulation. Endocrinology 142:3187–3197
15. **Conley AJ, Howard HJ, Slanger WD, Ford JJ** 1994 Steroidogenesis in the preovulatory porcine follicle. Biol Reprod 51:655–661
16. **Reinthaller A, Kirchheimer JC, Deutinger J, Bieglmayer C, Christ G, Binder BR** 1990 Plasminogen activators, plasminogen activator inhibitor, and fibronectin in human granulosa cells and follicular fluid related to oocyte maturation and intrafollicular gonadotropin levels. Fertil Steril 54:1045–1051
17. **Kroetz DL, Zeldin DC** 2002 Cytochrome P450 pathways of arachidonic acid metabolism. Curr Opin Lipidol 13:273–283
18. **Weintraub NL, Fang X, Kaduce TL, VanRollins M, Chatterjee P, Spector AA** 1999 Epoxide hydrolases regulate epoxyeicosanoic acid incorporation into coronary endothelial phospholipids. Am J Physiol 277:H2098–H2108
19. **Capdevila JH, Falck JR, Harris RC** 2000 Cytochrome P450 and arachidonic acid bioactivation. Molecular and functional properties of the arachidonate monooxygenase. J Lipid Res 41:163–181
20. **Zeldin DC** 2001 Epoxygenase pathways of arachidonic acid metabolism. J Biol Chem 276:36059–36062
21. **Summerer S, Hanano A, Utsumi S, Arand M, Schuber F, Blee E** 2002 Stereochemical features of the hydrolysis of 9,10-epoxystearic acid catalysed by plant and mammalian epoxide hydrolases. Biochem J 366:471–480
22. **Arand M, Knehr M, Thomas H, Zeller HD, Oesch F** 1991 An impaired peroxisomal targeting sequence leading to an unusual bicompartmental distribution of cytosolic epoxide hydrolase. FEBS Lett 294:19–22
23. **Hennebold JD, Tanaka M, Saito J, Hanson BR, Adashi EY** 2000 Ovary-selective genes. I. The generation and characterization of an ovary-selective complementary deoxyribonucleic acid library. Endocrinology 141:2725–2734
24. **Corbin CJ, Moran FM, Vidal JD, Ford JJ, Wise T, Mapes SM, Njar VC, Brodie AM, Conley AJ** 2003 Biochemical assessment of limits to estrogen synthesis in porcine follicles. Biol Reprod 69:390–397
25. **FASS** 1999 Guide for the care and use of agricultural animals in agricultural research and teaching. 1st ed. Savoy, IL: Federation of Animal Science Societies
26. **Li MD, DePaolo LV, Ford JJ** 1997 Expression of follistatin and inhibin/activin subunit genes in porcine follicles. Biol Reprod 57:112–118
27. **Corbin CJ, Trant JM, Conley AJ** 2001 Porcine gonadal and placental isozymes of aromatase cytochrome P450: sub-cellular distribution and support by NADPH-cytochrome P450 reductase. Mol Cell Endocrinol 172:115–124
28. **Moran FM, Ford JJ, Corbin CJ, Mapes SM, Njar VC, Brodie AM, Conley AJ** 2002 Regulation of microsomal P450, redox partner proteins, and steroidogenesis in the developing testes of the neonatal pig. Endocrinology 143:3361–3369
29. **Beetham JK, Tian T, Hammock BD** 1993 cDNA cloning and expression of a soluble epoxide hydrolase from human liver. Arch Biochem Biophys 305:197–201
30. **Wixtrom RN, Silva MH, Hammock BD** 1988 Affinity purification of cytosolic epoxide hydrolase using derivatized epoxy-activated Sepharose gels. Anal Biochem 169:71–80
31. **Borhan B, Mebrahtu T, Nazarian S, Kurth MJ, Hammock BD** 1995 Improved radiolabeled substrates for soluble epoxide hydrolase. Anal Biochem 231:188–200
32. **Newman JW, Watanabe T, Hammock BD** 2002 The simultaneous quantification of cytochrome P450 dependent linoleate and arachidonate metabolites in urine by high-performance liquid chromatography-tandem mass spectroscopy. J Lipid Res 43:1563–1578
33. **Gill SS, Ota K, Hammock BD** 1983 Radiometric assays for mammalian epoxide hydrolases and glutathione *S*-transferase. Anal Biochem 131:273–282
34. **DuTeaux SB, Newman JW, Morisseau C, Fairbairn EA, Jelks K, Hammock BD, Miller MG** 2004 Epoxide hydrolases in the rat epididymis: possible roles in xenobiotic and endogenous fatty acid metabolism. Toxicol Sci 78:187–195
35. **Smith DL, Willis AL** 1987 A suggested shorthand nomenclature for the eicosanoids. Lipids 22:983–986
36. **Smith WL, Gorgeat P, Hamberg M, Roberts II LJ, Willis AL, Yamamoto S, Ramwell PW, Rokach J, Sammuelsson B, Corey EJ, Pace-Asciak CR** 1990 Nomenclature. In: Murphy RC, Fitzpatrick FA, eds. Methods in enzymology. San Diego: Academic Press; 1–9
37. **Wixtrom RN, Hammock BD** 1985 Membrane-bound and soluble-fraction epoxide hydrolases: methodological aspects. In: Zakim D, Vessey DA, eds. Biochemical pharmacology and toxicology. New York: Wiley & Sons; 1–93
38. **Moody DE, Hammock BD** 1987 Purification of microsomal epoxide hydrolase from liver of rhesus monkey: partial separation of *cis-* and *trans-*stilbene oxide hydrolase. Arch Biochem Biophys 258:156–166
39. **Yu Z, Xu F, Huse LM, Morisseau C, Draper AJ, Newman JW, Parker C, Graham L, Engler MM, Hammock BD, Zeldin DC, Kroetz DL** 2000 Soluble epoxide hydrolase regulates hydrolysis of vasoactive epoxyeicosatrienoic acids. Circ Res 87:992–998
40. **Morisseau C, Beetham JK, Pinot F, Debernard S, Newman JW, Hammock BD** 2000 Cress and potato soluble epoxide hydrolases: purification, biochemical characterization, and comparison to mammalian enzymes. Arch Biochem Biophys 378:321–332
41. **Hedin L, Gaddy-Kurten D, Kurten R, DeWitt DL, Smith WL, Richards JS** 1987 Prostaglandin endoperoxide synthase in rat ovarian follicles: content, cellular distribution, and evidence for hormonal induction preceding ovulation. Endocrinology 121:722–731
42. **Davis BJ, Lennard DE, Lee CA, Tiano HF, Morham SG, Wetsel WC, Langenbach R** 1999 Anovulation in cyclooxygenase-2-deficient mice is restored by prostaglandin $E_2$ and interleukin-1$\beta$. Endocrinology 140:2685–2695
43. **Matsumoto H, Ma W, Smalley W, Trzaskos J, Breyer RM, Dey SK** 2001 Diversification of cyclooxygenase-2-derived prostaglandins in ovulation and implantation. Biol Reprod 64:1557–1565
44. **Curry Jr TE, Bryant C, Haddix AC, Clark MR** 1990 Ovarian prostaglandin endoperoxide synthase: cellular localization during the rat estrous cycle. Biol Reprod 42:307–316
45. **Yoshimura Y, Hosoi Y, Atlas SJ, Ghodgaonkar R, Dubin NH, Dharmarajan AM, Wallach EE** 1994 Inhibition of gonadotrophin-induced ovulation in rabbits by perfusion with dibutyryl cAMP via reduction of ovarian prostaglandin production. J Reprod Fertil 101:207–212

46. **Brannstrom M, Wang L, Norman RJ** 1993 Effects of cytokines on prostaglandin production and steroidogenesis of incubated preovulatory follicles of the rat. Biol Reprod 48:165–171

47. **Inoue N, Yamada K, Imai K, Aimoto T** 1993 Sex hormone-related control of hepatic epoxide hydrolase activities in mice. Biol Pharm Bull 16:1004–1007

48. **Nakagawa K, Marji JS, Schwartzman ML, Waterman MR, Capdevila JH** 2003 Androgen-mediated induction of the kidney arachidonate hydroxylases is associated with the development of hypertension. Am J Physiol 284:R1055–R1062

49. **Node K, Ruan XL, Dai J, Yang SX, Graham L, Zeldin DC, Liao JK** 2001 Activation of G$\alpha$s mediates induction of tissue-type plasminogen activator gene transcription by epoxyeicosatrienoic acids. J Biol Chem 276:15983–15989

50. **Szymanski W, Walentowicz M, Kotschy M** 2003 [Tissue-type plasminogen activator (T-PA) and plasminogen activator inhibitor (PAI-1) in human follicular fluid during gonadotropin-induced ovulation]. Ginekol Pol 74:1386–1391 (Polish)

51. **Li M, Karakji EG, Xing R, Fryer JN, Carnegie JA, Rabbani SA, Tsang BK** 1997 Expression of urokinase-type plasminogen activator and its receptor during ovarian follicular development. Endocrinology 138:2790–2799

52. **Zeldin DC, Moomaw CR, Jesse N, Tomer KB, Beetham J, Hammock BD, Wu S** 1996 Biochemical characterization of the human liver cytochrome P450 arachidonic acid epoxygenase pathway. Arch Biochem Biophys 330:87–96

53. **Holla VR, Makita K, Zaphiropoulos PG, Capdevila JH** 1999 The kidney cytochrome P-450 2C23 arachidonic acid epoxygenase is upregulated during dietary salt loading. J Clin Invest 104:751–760

54. **Yu Z, Huse LM, Adler P, Graham L, Ma J, Zeldin DC, Kroetz DL** 2000 Increased CYP2J expression and epoxyeicosatrienoic acid formation in spontaneously hypertensive rat kidney. Mol Pharmacol 57:1011–1020

55. **Scarborough PE, Ma J, Qu W, Zeldin DC** 1999 P450 subfamily CYP2J and their role in the bioactivation of arachidonic acid in extrahepatic tissues. Drug Metab Rev 31:205–234

56. **Wu S, Moomaw CR, Tomer KB, Falck JR, Zeldin DC** 1996 Molecular cloning and expression of CYP2J2, a human cytochrome P450 arachidonic acid epoxygenase highly expressed in heart. J Biol Chem 271:3460–3468

57. **Inouye K, Kondo S, Yamamura M, Nakanishi D, Sakaki T** 2001 Inhibitory effects of detergents on rat CYP1A1-dependent monooxygenase: comparison of mixed and fused systems consisting of rat CYP 1A1 and yeast NADPH-P450 reductase. Biochem Biophys Res Commun 280:1346–1351